Effects of localization on the excitonic linewidth in partially ordered $Ga_xIn_{1-x}P$ alloys

S. Smith,* Yong Zhang, A. Mascarenhas, and M. Hanna
National Renewable Energy Laboratory, Golden, Colorado 80401, USA
(Received 16 October 2003; revised manuscript received 8 April 2004; published 2 December 2004)

Spontaneous ordering in the ternary alloy $Ga_xIn_{1-x}P$ naturally leads to a reduction in alloy scattering and thus a reduction in the excitonic linewidth with increasing order parameter η. Concomitantly, the effect of localized states associated with various defects tends to increase the exciton linewidth, and it was observed that for $\eta \geqslant 0.45$, the linewidth actually *increases* with order parameter [Phys. Rev. B **61**, 9910 (2000)]. This was attributed to the increase in native defects which occurs for higher order parameters due to limitations in current growth technology. We show, using spatially resolved PL imaging with confocal and near-field microscopy, that this trend is reproduced in *all* ordered- $Ga_xIn_{1-x}P$ samples, within the micro-ensemble formed by the collection of all spectra in a spatially and spectrally resolved PL image, directly imaging the effect of exciton localization. This reversed trend is a result of the interplay between the effects of localization and spontaneous ordering, and the spatial averaging which occurs when examining areas many times larger than the exciton Bohr radius. Agreement with the trend observed in macro-PL is obtained via micro-ensemble averaging of each data set, and by examination of the spatial correlation of exciton linewidths. The implications of these results on the origin of the exciton linewidth in ordered alloys and the effect of ordering on the spatial distribution of exciton linewidths are discussed.

DOI: 10.1103/PhysRevB.70.235301 PACS number(s): 78.66.Fd, 71.55.Eq

I. INTRODUCTION

$Ga_xIn_{1-x}P$ ($x \cong 0.52$; written for the sake of simplicity as $GaInP_2$) is a substitutional alloy which exhibits spontaneous long range CuPt-type ordering, manifested as a monolayer superlattice of the alternating layers $Ga_{x+\eta/2}In_{x-\eta/2}P/Ga_{x-\eta/2}In_{x+\eta/2}P$ where η, known as the order parameter, is a statistical parameter that can vary between 0 and 1, depending on growth conditions.[1,2] The ordering leads to dramatic changes in the band structure: Including a large band-gap reduction,[3] valence-band splitting[4,5] and optical anisotropy.[4] As these properties are tunable by varying growth conditions, ordered- $GaInP_2$ has attracted interest for optoelectronic device applications.[6–8] From a more fundamental point of view, this material system is also well-suited to the study of the statistical effects of spontaneous ordering and the evolution from disorder to order in ordered alloys.[11,9,10]

Recently, we reported the effect of spontaneous ordering on the excitonic linewidth in partially ordered $GaInP_2$ alloys.[9] That is, a decrease in exciton linewidth with order parameter η, a consequence of the decrease in alloy scattering which results upon ordering. However, as mentioned in that work, the reverse trend was observed for samples with $\eta \geqslant 0.45$. For these samples, the exciton linewidth *increased* with order parameter. This was attributed to an increase in the density of native defects, such as anti-phase boundaries, which occurs for higher order parameters due to limitations in current growth technology.

In this paper, we examine the variations in exciton linewidth in a series of samples with sub-micron spatial resolution. When comparing the variation in exciton linewidth versus energy for a micro-ensemble consisting of the set of all points in each spatially resolved data set, this reversed trend is observed in *all* samples, albeit on a much finer energy scale than the macro-PL measurements of Ref. 9 (typically $\sim 1-4$ meV, compared to the ~ 140 meV spread in energies for η varying from 0 to roughly 0.5). This comes as a result of the interplay between the effects of localized states and the ordering induced reduction in alloy scattering, which always coexist in partially ordered alloys.

This effect uniquely highlights a nontrivial difference between measurements on macroscopic and sub-micron length scales in ordered alloys: While any optical measurement takes an ensemble average over the excitation volume, the trend revealed in these measurements is averaged-out and, therefore, lost in macro-PL measurements. Yet, examination of the spatial distribution of the exciton energy and linewidth on the sub-micron length scale gives insight into the origin of the inhomogeneous broadening observed in these alloys. Agreement with macro-PL is obtained via micro-ensemble averaging, and through examination of the spatial correlation in exciton linewidths. The implications of this effect on the origins of the inhomogeneous linewidth, and the effects of spontaneous ordering on the exciton linewidth in these alloys are discussed.

II. EXPERIMENT

The measurements were made using a low-temperature confocal microscopy/spectroscopy apparatus described in a previous publication,[12] where a spatial resolution of $\sim 0.7\mu$m was demonstrated. Excitation at 532 nm was imaged confocally onto the samples through an axial cryostat window and the photoluminescence was imaged in the reverse fashion and sent to a spectrometer/CCD. The samples were raster scanned and a series of spectra acquired. The corresponding energies and linewidths were found by computer analysis which used a least-squares fit to a Gaussian lineshape. For the near-field measurements, the same scanning system was further modified as a near-field scanning optical microscope, using the fiber probe developed by Betzig *et al.*[13] Spectra

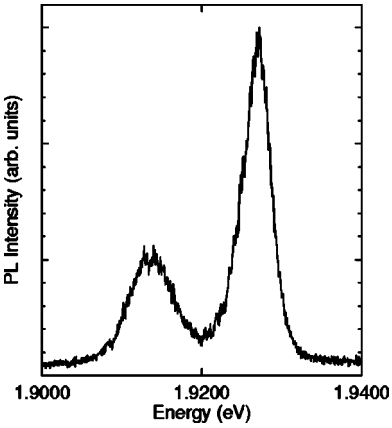

FIG. 1. Representative μ-PL spectra taken using the scanning confocal microscope for ordered- $GaInP_2$ sample with $\eta \sim 0.4$. High-energy peak is inhomogeneously broadened (near) band-edge exciton. The origin of the lower energy peak is still debated, but believed to be defect-related.

were collected in a shared-aperture mode, exciting and collecting emission through the 200 nm aperture of the fiber tip, similar to the measurements described in Ref. 14. In both the confocal and near-field setups, the shared aperture geometry minimizes the effects of diffusion on image resolution. The estimated excitation density varied between 0.1 and 10 W/cm^2, depending on the technique and excitation spot-size. As noted in Ref. 9, it was observed that the linewidth in these samples did not change as the power was varied up to 40 W/cm^2. We, therefore, do not believe these results are influenced by variations in excitation density. All measurements were made at 5 K. The samples were all single-variant $CuPt_B$-type ordered $GaInP_2$ with order parameter η varied from ~ 0 to 0.45.

III. RESULTS

Figure 1 shows a representative spectra taken at 5 K using the confocal apparatus. The high energy peak has been identified previously as the (near) band-edge excitonic peak by photoluminescence (PL) and photoluminescence excitation spectroscopy (PLE).[4,15] The origins of the low-energy peak are less clear, but are commonly believed to be defect related. In random alloys, and partially ordered alloys like $GaInP_2$, the exciton is assumed to be weakly localized due to alloy disorder, and theoretical treatments typically neglect exciton center-of-mass motion.[9,16,17] This is evidenced by the substantial stokes shift observed between PL and PLE in these alloys (e.g., ~ 10 meV for the sample in Ref. 15). With typical linewidths in the range of 4–6 meV full width at half maximum (FWHM) for even the highest-quality samples obtainable, this peak is well described by an inhomogeneously broadened Gaussian line shape. Thus the significance in examining the spatial variations in excitonic peak energy and linewidth in these materials is to understand the origins of this inhomogeneous broadening and their relation to the effect of spontaneous ordering.

Figure 2(a) shows the spatial variation in the excitonic peak energy over a 5.5 μm square region in a $GaInP_2$ epilayer with $\eta \sim 0.39$, Fig. 2(b) shows the corresponding spatial variation in linewidth. It can be seen by inspection that regions of lower peak energy correspond to regions of relatively broader linewidth. This trend is also reproduced in the scatter plot of linewidth vs energy for the same data set, shown in Fig. 2(c). The trend illustrated in Fig. 2(c) is reproduced in all the samples of this study, and previous μ-PL measurements.[11] This plot shows the exciton linewidth *increasing* with decreasing energy, exactly opposite the effect observed in Ref. 9. Naively, one may expect that if the subtle variations in exciton energy observed in spatially resolved images were due solely to variations in order-parameter η, then the trend observed in the macro-PL measurements of Ref. 9 would be reproduced on a smaller energy-scale within each spatially resolved data set. As this is not observed, it becomes clear that the linewidth must have at least two contributions:

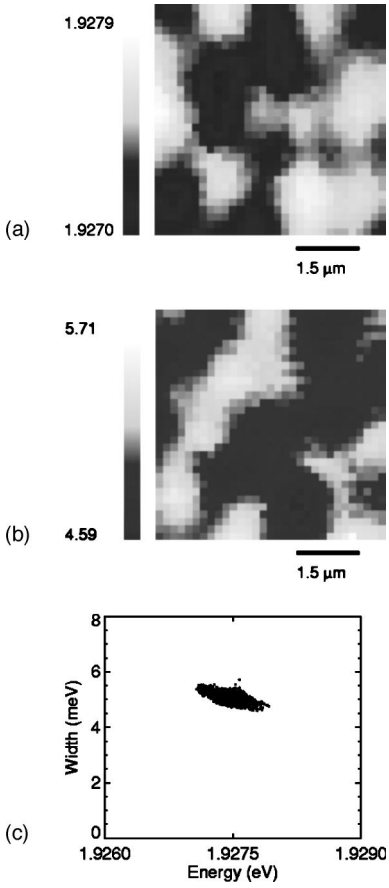

FIG. 2. (a): Spatial map of excitonic energy, (b): Corresponding map of exciton linewidth, and (c): Scatterplot of linewidth vs energy for sample with $\eta \sim 0.39$. Energy and linewidth grey scales are in eV and meV, respectively.

$$\sigma(x,y,\eta) = \sqrt{\sigma^2_{\text{global}}(\eta) + \sigma^2_{\text{local}}(x,y)} \tag{1}$$

where σ_{global} corresponds to the contribution due to alloy scattering, as discussed in Ref. 9, and σ_{local} the contribution due to local fluctuations, as directly imaged in Figs. 2(a) and 2(b), whose dependence on energy (and thus order parameter η) contradicts that of σ_{global}. These local variations are

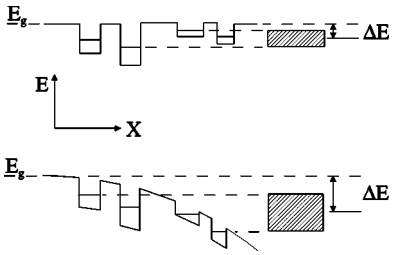

FIG. 3. Above: Random potential fluctuations localize excitons over a range of energies, giving rise to the inhomogeneous linewidth, represented by the height of the greyed box. Below: the presence of longer length-scale potential fluctuations increases the spread in excitonic energies and the shift in the average excitonic peak energy with respect to the band gap (labeled ΔE).

averaged-out in macro-PL measurements, adding an offset to the intrinsic linewidth for a given composition and order-parameter. The possible origins of σ_{local} will be discussed later, at this point it is important to point out that the trend observed in Fig. 2(c) cannot be explained by spatial variations in order parameter, and therefore, such sub-micron variations in exciton energy should not be interpreted as stemming solely from variations in η.

The spatial-resolution of these measurements, while sub-micron, still includes thousands of exciton volumes, and therefore, constitutes a spatial average over the local environment. As seen in Fig. 3, this affects both the measured linewidth and the peak energy: The upper portion of the figure shows a schematic representation of the random spatial distribution of localized states which are presumed to exist in the partially ordered alloys. The range of energies within the spatial region being sampled should, in principle, give rise to the inhomogeneously broadened linewidth observed. The spatial average of these energies, weighted by the relative intensities of each localized state, gives the measured average energy and peak position observed. The presence of a longer length-scale potential fluctuation (that is, much larger than the exciton Bohr radius), as shown in the lower part of the figure, would necessarily increase the spread in energies observed (and thus the linewidth) as well as shift the measured average energy (the observed peak position).

This effect should depend on both the strength of the potential fluctuation and the spatial extent of the measurement (the coordinate *X* in Fig. 3). A data set similar to that shown in Fig. 2, was generated for a sample with $\eta \sim 0.38$ using a low-temperature near-field microscope, the results of which are shown in Fig. 4. Here, the spatial extent of the measurement is $\approx$200 nm, 3.5 times smaller than the confocal technique (spot size $w \sim 0.7 \mu$m). The measured linewidths shown in Fig. 4(b) are about 1 meV smaller than those shown in Fig. 2(b), though the order parameter is nearly equal in this case, consistent with the above discussion. Figure 5 shows the spatial maps of energy and linewidth for the sample with $\eta \sim 0.45$, with the same spatial resolution as that in Fig. 2. The total variation in exciton energies is much greater than for the sample with $\eta \sim 0.39$ (shown in Fig. 2). The ensemble-averaged linewidth for this sample, $\sim$6.5 meV (as discussed later in relation to Fig. 7), is commensurately broadened. Also seen in the spatial map of line-

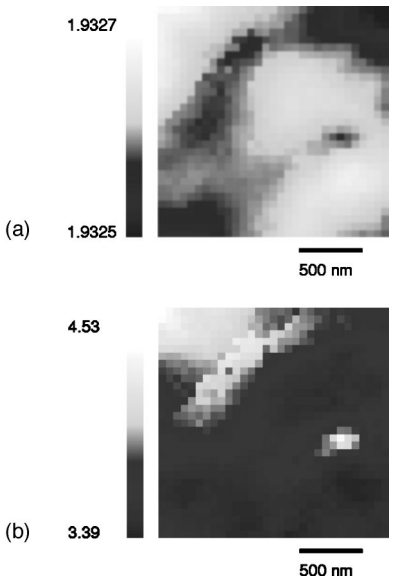

FIG. 4. Spatial map of excitonic energy (a) and exciton linewidth (b) obtained using near-field microscopy with $\approx$3.5x smaller spot size ($\approx$200 nm) for sample with $\eta \sim 0.38$. Energy and linewidth spatial map grey scales are in eV and meV.

widths shown in Fig. 5(b), localized states are strongly broadened, again directly imaging the effects of localization. The spatial extent of the measurement corresponds to the spatial resolution of the confocal technique, verified to be $\approx 0.7\ \mu$m.[12] This again is consistent with the above-mentioned picture: For a fixed spot-size, the observed linewidth should increase with the spread in energies.

A unique feature of the spatially resolved measurements is that, because of the large number of spectra taken in each image ($\sim$1000), it allows to examine the statistical distribution of the exciton energy, which in turn offers insights into

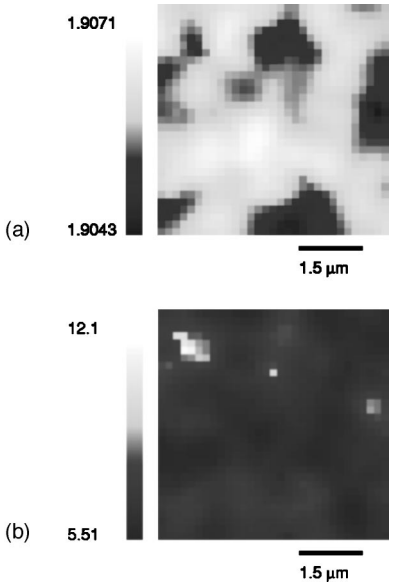

FIG. 5. Spatial map of excitonic energy (a) and exciton linewidth (b) obtained for sample with $\eta \sim 0.45$, taken with the confocal setup. Energy and linewidth grey scales are in eV and meV.

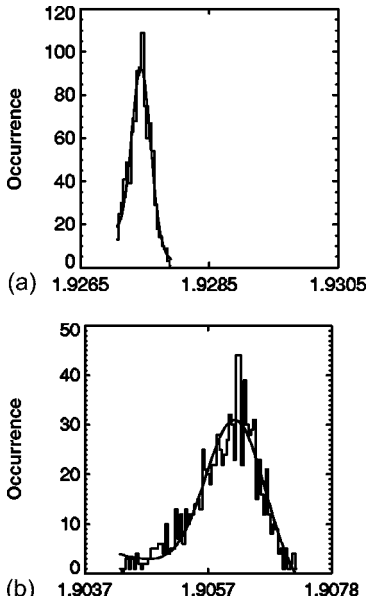

FIG. 6. (a) Histogram of exciton energies for data set shown in Fig. 2(a) (solid line is least-squares fit to a Gaussian distribution). (b) Histogram of exciton energies for data set shown in Fig. 5(a) and corresponding least-squares fit to Gaussian function. Note the histogram shown in (b) is asymmetric and skewed toward the low-energy side, an effect of localization.

the origin of the exciton linewidth in these alloys. Figure 6 shows a comparison of the histograms generated with the data of Figs. 2 and 5. The distribution shown in Fig. 6(a) seems reasonably symmetric and, therefore, consistent with the random statistics expected for substitutional alloys. The distribution shown in Fig. 6(b), however, is noticeably skewed toward lower energies, with a pronounced low-energy tail, indicative of localized states. Thus the linewidth in this case is dominated by these localized states and the effects of localization, which overcome the ordering induced linewidth reduction. This is born out by examining the micro-ensemble averaged energy vs linewidth shown in Fig. 7, and discussed in the following paragraph.

By examining the statistical distribution in exciton energy and linewidth, micro-ensemble averages can also be formed. Figure 7 shows a plot of micro-ensemble averaged excitonic energy vs linewidth for all the samples studied. Also plotted for reference is the order parameter, related to the excitonic energy, as in Ref. 2. It can be seen that the excitonic linewidth decreases with increasing η / decreasing energy, as in the macroscopic PL measurements reported earlier,[9] with the exception of the sample with $\eta \sim 0.45$, for which the linewidth broadening effect discussed above overcomes the ordering induced linewidth reduction.

Further insights into the origin of the observed submicron variations in the excitonic linewidth can be found by examining the spatial correlation of excitonic linewidths. This is the average distance after which the linewidth at two locations $\overline{r}$ and $\overline{r'}$ become 50% uncorrelated. This length can be extracted by computing the two-dimensional spatial correlation function defined as:

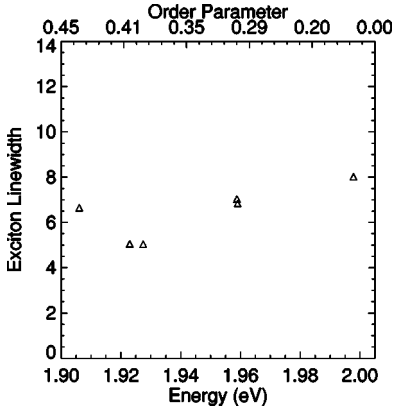

FIG. 7. Scatter plot of ensemble-averaged energy and linewidth of all samples studied. The average linewidth decreases with increasing order parameter/decreasing band-gap energy. For the sample with $\eta \sim 0.45$, the effects of localization overcome the ordering induced linewidth reduction.

$$\overline{C}_{\sigma\sigma'}(\overline{r}-\overline{r'}) = \frac{1}{N}\sum_{i,j} \sigma(\overline{r_{ij}})\sigma(\overline{r_{ij}}-\overline{\Delta})/\sigma(\overline{r_{ij}})^2$$

Where $\sigma(\overline{r})$ is the linewidth at each point in the plane, N is the total number of data points in the plane, ij are coordinate indices which represent each point in the scan plane and $\overline{\Delta} = \overline{r}-\overline{r'}$. Figure 8 shows a one-dimensional line cut of this function which passes horizontally through the two-dimensional peak at $\overline{\Delta}=0$ (the full two-dimensional function for the first data set is shown in a greyscale plot in the inset of the figure). This is plotted for each of the samples whose linewidth dependence on ordering was not overcome by localization effects (as discussed earlier). The initial decay of this function characterizes how rapidly the linewidth changes with distance, the behavior of this function at larger $\overline{\Delta}$ is less clear, but likely depends on extrinsic details of the particular region of the sample examined and the effects of finite size on the computation. The half width at half maximum of the

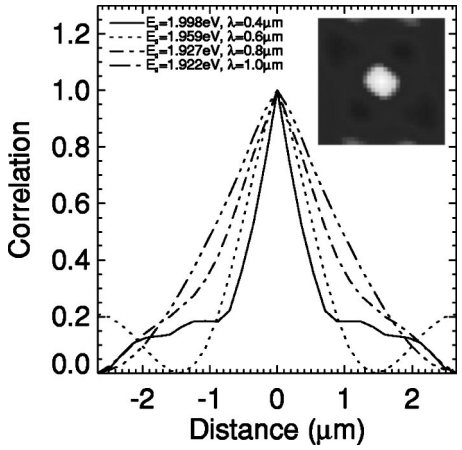

FIG. 8. Linecuts of the 2D correlation function $C_{\sigma\sigma'}(\overline{r}-\overline{r'})$ for samples with order parameter $\eta \sim 0-0.41$. The full 2D function for the first data set is plotted in greyscale and shown in the inset.

symmetric peaks for each of these samples corresponds to the correlation length. A clear trend is observed, the correlation length increases from 0.4 to 1.0 μm as the band-gap energy decreases from 1.998 to 1.927 eV (order parameter η varies from $\sim$0 to 0.41).

This behavior can be interpreted in the following way: For a disordered alloy, the local alloy composition should exhibit random alloy fluctuations. If these statistical fluctuations are random, they should exhibit a so-called white frequency spectrum, including fluctuations at all length scales. The exciton will average the alloy composition over its Bohr radius, thus the highest spatial frequencies are washed out by the exciton itself. Fluctuations on length scales less than the spatial resolution are similarly averaged out due to fluctuations in alloy composition seen by excitons in various locations within the sampled volume. Therefore, it is only the fluctuations on length scales greater than the spatial resolution that are observed to influence the spatial variations in linewidth seen in these measurements. It is observed that these fluctuations, if due to intrinsic alloy fluctuations, tend to decrease with the degree of ordering. As the alloy becomes increasingly ordered, this average exciton energy must become increasingly uniform, as we expect the linewidth in a perfectly ordered alloy to be translationally invariant. Therefore, the linewidth correlation length should also increase upon ordering, as is observed. We expect the existence of the observed spatial variations in exciton linewidth, as well as the increase in correlation length, should be a natural consequence of the transition from disorder to order in partially ordered alloys.

IV. DISCUSSION

The origin of the exciton linewidth in substitutional alloys is primarily due to alloy fluctuations within the exciton volume. As was shown in Ref. 9, spontaneous ordering in $GaInP_2$ reduces the randomness of the alloy and consequently reduces the exciton linewidth. In PL measurements, the exciton acts as a probe of alloy fluctuations. If these fluctuations are on a finer length scale than the exciton Bohr radius, the linewidth should be independent of the volume of material probed. Yet linewidths observed in this work as well as other micro-PL measurements[11] indicate inhomogeneity on length scales much greater than the exciton Bohr radius. Theoretical treatments commonly assume the exciton is fully localized and thus neglect center-of-mass motion.[9,16,17] Obviously, as the alloy becomes increasingly ordered, the assumption of zero center-of-mass motion must break down. Likewise, the randomness of the alloy must "anneal out" with increasing η. Thus there must be a smooth transition from a random alloy to a fully ordered alloy. The observation that the observed linewidth depends on the spatial resolution, and the dependence of the spatial linewidth correlation length on order parameter η, suggest that longer length-scale fluctuations must appear as a consequence of spontaneous ordering and the transition from disorder to a fully ordered alloy.

Simultaneously, ordering-related defects such as those associated with anti-phase boundaries and the polarization fields predicted to develop in these alloys[18] must give rise to localized states which tend to broaden the exciton linewidth through both their influence on the exciton binding energy and possible confinement effects,[19–21] and through the spatial averaging effects discussed in this work. Estimating the contribution due to this is difficult, as the contributions of σ_{global} and σ_{local} to the exciton linewidth are difficult to distinguish. Still, spatially resolved measurements such as the ones discussed here offer the best hope of doing this. If one assumes that σ_{global} can be identified as the minimum linewidth in a spatially resolved data set, the contribution due to σ_{local} can be obtained from Eq. (1). For instance, for the deepest fluctuation in the data set shown in Fig. 2, $\sigma_{\text{local}}=3.3$ meV. As the material becomes increasingly ordered, excitons move more freely and therefore are more likely to find deep potential minima. Thus ordering can amplify the effect of defects on the exciton linewidth, as in the case of the dataset shown in Fig. 5. As evidenced by the localization tail in the exciton energy distribution for this sample, shown in Fig.6(b), the linewidth in this sample has a strong contribution from localized, defect-related states. As a result of this, the ensemble-averaged linewidth, which closely approximates macro-PL measurements, is strongly affected by these states.

The reversed-dependence of linewidth on energy observed within the micro-ensemble shown in Fig. 2(c) is likely another localization effect. As measurements of this kind are rare, no theoretical treatment yet exists. Yang *et al.* showed that the distribution of potential minima in a 2D-Gaussian distribution of energy states is also Gaussian, resulting in a universal constant of proportionality between the Stokes shift observed in PL and the absorption linewidth in quantum wells.[22,23] Their result is independent of the details of the quantum well, resulting from the assumption of an energy surface characterized by Gaussian statistics in a planar sample. A similar relation has been observed in II-VI substitutional alloys, where the stokes shift is linearly proportional to the characteristic energy of the band-tail density of states ($\epsilon_\circ$) for excitons localized by compositional disorder.[24] Reference 25 extends the work of Singh and Bajaj[26] to analyze the lineshape of weakly localized excitons in II–VI alloys, and directly calculates the lineshape as a function of this characteristic energy. The simulated and experimental data in this work also show the trend of increasing emission linewidth with decreasing energy (increasing ϵ, measured from the free exciton energy). As each data point in the scatterplot shown in Fig. 2(c) can be considered an ensemble average on the 100's of nanometer lengthscale, the linewidth and energy of the measured peak can be considered as a measure of the local remnant disorder in the partially ordered alloy. While such variations may be small, examination of their spatial distribution and corresponding correlation lengths gives insight into the process of spontaneous ordering and the effects of disorder on the exciton linewidth. In contrast, larger fluctuations, such as those shown in Fig. 5 and the corresponding non-Gaussian tail of the histogram shown in Fig. 6 are likely defect related.

V. SUMMARY

In summary, the spatial variation in excitonic energy and linewidth were studied using low-temperature confocal and

near-field microscopy / spectroscopy in a series of partially ordered $Ga_xIn_{1-x}P$ alloys ($x \approx 0.52$), with varying order parameter $\eta \sim 0-0.45$. The disorder-related effects of exciton localization on the excitonic line shape were directly observed through spectroscopic imaging and line shape analysis. The data show the effect of spatial averaging over multiple localized states and its dependence on the spatial extent of the measurement. Surprisingly, the exciton linewidth was observed to *increase* with decreasing energy (increasing order parameter η) within the micro-ensemble formed by the set of all points in each spatially resolved image, contrary to the previously reported trend observed in macro-PL measurements. Agreement with macro-PL is retrieved via a micro-ensemble average of each data set. The dependence of the spatial correlation length of the exciton linewidth on ordering was observed, and found to increase with order parameter for samples whose linewidth dependence on ordering was not overcome by localization effects; indicating the presence of long-wavelength fluctuations in the disorder potential, which statistically lengthen with order parameter. Measurements such as these help characterize the transition from disorder to order, and elucidate the mechanisms which affect the inhomogeneous linewidth in spontaneously ordered alloys, on a length scale not previously observed.

ACKNOWLEDGMENT

This work was supported by US-DOE Office of Science, Material Science Division, Contract No. DE-AC36-83CH10093.

*Electronic address: steven_smith@nrel.gov

[1] S.-H. Wei and A. Zunger, Appl. Phys. Lett. **56**, 662 (1990).
[2] Yong Zhang, Angelo Mascarenhas, and Lin-Wang Wang, Phys. Rev. B **63**, 201312 (R) (2001).
[3] A. Gomyo and T. Suzuki, Phys. Rev. Lett. **60**, 2645 (1988).
[4] A. Mascarenhas, S. Kurtz, A. Kibbler, and J. M. Olson, Phys. Rev. Lett. **63**, 2108 (1989).
[5] S.-H. Wei, D. B. Laks, and A. Zunger, Appl. Phys. Lett. **62**, 1937 (1993).
[6] K. H. Huang, J. G. Yu, C. P. Kuo, R. M. Fletscher, T. D. Osentwski, L. J. Stinson, M. G. Craford, and A. S.H. Liao, Appl. Phys. Lett. **61**, 1045 (1992).
[7] H. Fujii, Y. Ueno, A. Gomyo, K. Endo, and T. Suzuki, Appl. Phys. Lett. **61**, 1959 (1992).
[8] K. A. Bertness, S. R. Kurtz, D. J. Friedman, A. E. Kibbler, C. Kramer, and J. M. Olson, Appl. Phys. Lett. **65**, 989 (1994).
[9] Yong Zhang, A. Mascarenhas, S. Smith, J. F. Geisz, J. M. Olson, and M. Hanna, Phys. Rev. B **61**, 9910 (2000).
[10] Yong Zhang, Angelo Mascarenhas, and Lin-Wang Wang, Phys. Rev. B **64**, 125207 (2001).
[11] H. M. Cheong, A. Mascarenhas, J. F. Geisz, J. M. Olson, M. W. Keller, and J. R. Wendt, Phys. Rev. B **57**, R9400 (1998).
[12] S. Smith, H. M. Cheong, B. D. Fluegel, J. F. Geisz, J. M. Olson, L. L. Kazmerski, and A. Mascarenhas, Appl. Phys. Lett. **74**, 706 (1999).
[13] E. Betzig, J. K. Trautman, T. D. Harris, J. S. Weiner, and R. L. Kostelak, Science **251**, 1468 (1991).
[14] S. Smith, A. Mascarenhas, S. P. Ahrenkiel, M. C. Hanna, and J. M. Olson, Phys. Rev. B **68**, 035310 (2003).
[15] P. Ernst, C. Geng, F. Sholz, H. Schweizer, Yong Zhang, and A. Mascarenhas, Appl. Phys. Lett. **67**, 2347 (1995).
[16] R. Zimmerman, J. Cryst. Growth **101**, 346 (1990).
[17] K. K. Bajaj, Mater. Sci. Eng., R. **34**, 59–120 (2001).
[18] Sverre Froyen, Alex Zunger, and A. Mascarenhas, Appl. Phys. Lett. **68**, 2852 (1996).
[19] G. Bastard, C. Delanlande, M. H. Meynadier, P. M. Frijlink, and M. Voos, Phys. Rev. B **29**, 7042 (1984).
[20] C. I. Harris, B. Monemar, H. Kalt, P. O. Holtz, M. Sundaram, J. L. Merz, and A. C. Gossard, Phys. Rev. B **51**, 13221 (1995).
[21] M. Bayer, S. N. Walck, T. L. Reinecke, and A. Forchel, Phys. Rev. B **57**, 6584 (1998).
[22] Fang Yang, M. Wilkinson, E. J. Autin, and K. P. O'Donnell, Phys. Rev. Lett. **70**, 323 (1993).
[23] A. Polemeni, A. Patanè, M. Grassi Alessi, M. Capizzi, F. Martelli, A. Bosacchi, and S. Franchi, Phys. Rev. B **54**, 16389 (1996).
[24] S. Permogorov and A. Reznitsky, J. Lumin. **52**, 201–223 (1992).
[25] Djamel Oudjaout and Yves Marfaing, Phys. Rev. B **41**, 12096 (1990).
[26] J. Singh and K. K. Bajaj, Appl. Phys. Lett. **48**, 1077 (1986).